CONF-840910--8

UCRL-90396
PREPRINT

UCRL--90396

DE84 015955

THERMAL BARRIER CONFINEMENT EXPERIMENTS IN THE TMX-U TANDEM MIRROR

T.C. Simonen, S.L. Allen, D.E. Baldwin, T.A. Casper, J.F. Clauser, F.H. Coensgen, R.H. Cohen, D.L. Correll, W.F. Cummins, C.C. Damm, J.H. Foote, T.K. Fowler, R.K. Goodman, D.P. Grubb, D.N. Hill, E.B. Hooper, R.S. Hornady, A.L. Hunt, R.G. Kerr, G.W. Leppelmeier, J.Marilleau, J.M. Moller, A.W. Molvik, W.E. Nexsen, J.E. Osher, W.L. Pickles, P. Poulsen, G.D. Porter, E.H. Silver, B.W. Stallard, J. Taska, W.C. Turner J.D. Barter, T.W. Christensen, G. Dimonte, T.E. Romesser R.F. Ellis, R.A. James, C.J. Lasnier T.L. Yu, L.V. Berzins, M.R. Carter, C.A. Clower, B.H. Failor, S. Falabella, M. Flammer, T. Nash, and W.L. Hsu

This paper was prepared for submittal to the
IAEA 10th International Conference on Plasma Physics and Controlled Nuclear Fusion Research
London, England, Sept. 12-19, 1984

July 26, 1984

INTERNATIONAL ATOMIC ENERGY AGENCY

TENTH INTERNATIONAL CONFERENCE ON PLASMA PHYSICS AND CONTROLLED NUCLEAR FUSION RESEARCH

London, UK, 12–19 September 1984

IAEA-CN-44/C-I-1

THERMAL BARRIER CONFINEMENT EXPERIMENTS IN THE TMX-U TANDEM MIRROR*

T.C. SIMONEN, S.L. ALLEN, D.E. BALDWIN, T.A. CASPER, J.F. CLAUSER, F.H. COENSGEN, R.H. COHEN, D.L. CORRELL, W.F. CUMMINS, C.C. DAMM, J.H. FOOTE, T.K. FOWLER, R.K. GOODMAN, D.P. GRUBB, D.N. HILL, E.B. HOOPER, R.S. HORNADY, A.L. HUNT, R.G. KERR, G.W. LEPPELMEIER, J.MARILLEAU, J.M. MOLLER, A.W. MOLVIK, W.E. NEXSEN, J.E. OSHER, W.L. PICKLES, P. POULSEN, G.D. PORTER, E.H. SILVER, B.W. STALLARD, J. TASKA, and W.C. TURNER
Lawrence Livermore National Laboratory,
University of California
Livermore, CA

J.D. BARTER, T.W. CHRISTENSEN, G. DIMONTE, and T.E. ROMESSER
TRW Corporation
Redondo Beach, California

R.F. ELLIS, R.A. JAMES, and C.J. LASNIER
University of Maryland
Baltimore, Maryland

T.L. YU
Johns Hopkins University
Baltimore, Maryland

L. V. BERZINS, M. R. CARTER, C. A. CLOWER, B. H. FAILOR, S. FALABELLA, M. FLAMMER, and T. NASH
University of California-Davis
Davis, California

W. L. HSU
Sandia National Laboratory
Livermore, California

United States of America

*Work performed under the auspices of the U.S. Department of Energy by the Lawrence Livermore National Laboratory under contract number W-7405-ENG-48.

ABSTRACT

THERMAL BARRIER CONFINEMENT EXPERIMENTS IN THE TMX-U TANDEM MIRROR

In our recent experiments on the TMX-U thermal-barrier device, we achieved the end plugging of axial ion losses up to a central cell density of $n_c = 6 \times 10^{12}$ cm^{-3}. During lower density experiments, we measured the axial potential profile characteristic of a thermal barrier and found an ion-confining potential greater than 1.5 kV and a potential depression of 0.45 kV in the barrier region. The average beta of hot end plug electrons has reached 15% and of hot central cell ions has reached 6%. In addition, we heated deuterium ions in the central cell with ICRF to an average perpendicular energy of 2 keV. During strong end plugging at low density (7×10^{11} cm^{-3}), the axial ion confinement time $\tau_{\parallel}$ reached 50 to 100 ms while the nonambipolar radial ion confinement time $\tau_{\perp}$ was 14 ms--independent of end plugging. Electrically floating end walls increased the radial ion confinement time by a factor of 1.8. At higher densities and lower potentials, $\tau_{\parallel}$ was 6 to 12 ms and $\tau_{\perp}$ exceeded 100 ms.

1. INTRODUCTION

The Tandem Mirror Experiment-Upgrade (TMX-U) is the first thermal-barrier tandem mirror to operate. Our recent experimental results demonstrate the formation of microstable sloshing-ion distributions [1,2], end plugging with a density larger in the central cell than the end plug, and formation of thermal barrier axial potential profile [3]. Additional work has shown the following: a continuing increase of hot electron beta up to 15% when we increase electron-cyclotron resonant heating (ECRH) power [4], heating of the central cell ions with ion-cyclotron resonant frequency (ICRF)[5], and decreasing radial ion transport with end wall potential control [6].

The TMX-U magnetic-field configuration consists of a 8-m-long 0.3-T solenoidal central cell, terminated at each end by a 3-m-long 0.5-T quadrupole mirror cell that performs the dual role of providing a thermal barrier potential profile for axial confinement as well as a magnetohydrodynamic (MHD) anchor.

Six 20-kV neutral beams, which are injected in the end plugs at 47° to the magnetic field lines, form sloshing-ion distributions and pump trapped ions out of the thermal

barriers. In each end plug, a 200-kW 28-GHz gyrotron heats electrons near the second harmonic resonance at the bottom of the magnetic well to create the thermal barrier; a second gyrotron at the fundamental resonance (ω_{ce}) locally heats electrons between the bottom of the well and the outside mirror to create the ion confining potential peak. Central cell ions are heated by two 200-kW ICRF antennas and by seven neutral beam injectors. The plasma is fueled by injecting gas in the central cell.

2. MEASUREMENTS OF THE THERMAL BARRIER POTENTIAL

Using three electrostatic analyzers with grids [7] located at the ends of the TMX-U, we measured the thermal barrier potential profile shown in Fig. 1b. Sloshing beams and ECRH heating were applied in the standard manner to create an end-plugging plasma in the west end cell (Fig. 1a). To make this measurement, we used only second harmonic ECRH in the east end cell; therefore, no potential peak or end plugging occurred in the east end cell. To measure the barrier potential ($\phi_e - \phi_b$) shown in Fig. 1b in the west end cell, we injected a diagnostic neutral beam at an 18° angle to the magnetic axis. The ionized-diagnostic-beam atoms stream along magnetic field lines out the east end of the machine. Their energy shift, measured by the analyzer ELA1, gives a direct measure of the barrier potential. The analyzers labeled ELA2 and ELA3 were swept through a lower energy range--from ground to 2.4 keV. Ions detected by these analyzers have a minimum energy ϕ_e (ELA2) or ϕ_p (ELA3), as determined by the decrease in ion current when the ion-repeller-grid voltage was swept through these values of potential. The peak potential height ϕ_p was not resolved because ions lost out the west end had energies greater than the maximum grid bias of 2.4 kV. Therefore, the central cell ion-confining potential $\phi_c = \phi_p - \phi_e$ exceeded 1.5 kV.

Several additional facts supporting the existence of a thermal barrier are as follows:

1. Non-Maxwellian plug electrons with bulk "temperature" exceeding central cell temperature;
2. Potential peak was enhanced by ECRH;
3. Rapid rise of end loss when plug ECRH was turned off;
4. End plugging required both sloshing ions and ECRH;
5. Axial confinement was improved;
6. End plugging was observed with $n_c > n_p$;
7. Plugging required hot electrons;
8. No plugging occurred unless central cell ions were sufficiently hot.

A remarkable feature of these thermal barrier experiments is that both the energetic ions and electrons remain stable to ion- and electron-cyclotron modes. Although weak fluctuations are detected, we have not observed degradation in confinement

resulting from either ion or electron modes. In our experiments, impurity concentrations (C,N,O) were also low, $\leq$1%.

3. PLASMA CONFINEMENT

The potential peaks in the end plugs reduce the axial loss of central cell ions when both ECRH (Fig. 1c) and sloshing ions (Fig. 1d) are present. Figure 1e shows end-loss currents out one end when both ends are plugged (the other end is similar). The pulsed nature of the end-loss current seen in Fig. 1e results from sweeping the analyzer ion-repeller voltage to measure the energy distribution. When the ion-repeller voltage exceeds the plasma potential plus a few times the central cell ion temperature, almost no ions reach the collector and the remaining signal is a negative current of energetic electrons that pass through the -2.0-kV electron-repeller grid. Using a second analyzer to measure the electron current, we determined that the ion axial-confinement time was at least 100 ms.

We determine the nonambipolar radial ion-confinement time $\tau_\perp$ by measuring the net current collected on the end walls. Negative currents, implying that the axial current of electrons exceeds that of ions, are measured. To preserve charge balance, we assume that there is an equal radial current of ions. This radial current value is used to calculate $\tau_\perp$.

The experimental scaling of $\tau_\perp$ with the central cell density (n_c) and the potential of the central cell plasma relative to ground (ϕ_e) are shown in Fig. 2 over a wide range of conditions. In Fig. 2a, above ϕ_e = 150 V, $\tau_\perp$ decreases as ϕ_e^{-2}; whereas at lower potentials $\tau_\perp$ is equal to 0.1 to 0.2 s. The region of ϕ_e^{-2} scaling begins near the resonance between the ion axial bounce and azimuthal E x B drift motions, where resonant transport theory predicts a general increase in radial transport [8]. The measured $\tau_\perp$ is less than predicted by theory by a factor 1 to 3. Overall, our experiments show the importance of avoiding operation at excessively high values of potential (relative to the ion and electron temperatures, as predicted by theory). Figure 2b shows that $\tau_\perp$ reaches 100 ms at densities above 10^{12} cm^{-3} when the potential is lower. There is less correlation of $\tau_\perp$ with n_c than with ϕ_e.

The average hot electron beta increases with ECRH power to 15% (30% locally on axis). After ECRH turnoff, the diamagnetic hot electron signal initially decays with a 10 to 20 ms decay rate, which later increases to 100 ms. The central cell beta, resulting mainly from the neutral beam injected ions, reaches 6% averaged over the radius to the limiter. Because the hot ions are undoubtedly localized in the plasma core, the on-axis beta is several times higher. The hot ions diamagnetic decay time is usually 3 to 5 ms, which is believed to be limited mainly by charge exchange on cold gas.

4. POTENTIAL CONTROL

Because of its nonambipolar nature and its relation to central cell potential, radial ion transport is amenable to control by adding conducting plates to the end walls of the machine; these may be either electrically floated or biased.

Results from our first experiments using potential control on TMX-U are shown in Fig. 3. In this arrangement (Fig. 3a), two end wall electrodes at each end of the device may be either electrically floated and the voltage measured, or switched to ground and the current measured. The inner elliptical disc maps to a 9.8-cm radius in the central cell, whereas the outer electrode extends to 12.9 cm. Because the actual plasma extends to 25 cm, these plates only influence the plasma core.

In Fig. 3b, the end plates are floating (-1200 V on the inner plates--similar to the central cell potential) until t = 35 ms when they are grounded. Because the plasma sources are fixed, the fact that the exponential build-up rate decreases as the plates are shorted is clear evidence of superior confinement while the plates are floating. The nonambipolar radial confinement time increased from 5.6 to 10.3 ms with the plates floating, a factor of 1.8. Additional evidence of improved radial confinement is the narrower radial-density profile before these plates are shorted (Fig. 3c).

Additional data taken by separately grounding the inner and outer electrodes show that suppressing the negative current corresponds to a decrease in the outward radial ion current rather than an increase in the outward radial electron current.

5. THERMAL BARRIER SCALING

Since the first observation of end plugging in TMX-U in February 1983, the central cell density n_c has been steadily increased with vacuum improvements [9] and with higher levels of ICRF and ECRH heating power from 1.5×10^{11} to 6×10^{12} cm^{-3}. Our goal is 2×10^{13} cm^{-3}. In this section we describe two thermal barrier scaling relations.

The central cell density and temperature must be increased concurrently to avoid excessive collisional trapping of the ions and charge neutralizing of the warm electrons in the thermal barrier region. In TMX-U trapped ions are removed by charge-exchange pumping, which occurs when we inject approximately 100 atom A of neutral beam current into each end plug. Equilibrium between the collisional filling and charge-exchange pumping determines the lines of constant $n_c/T_{ic}^{3/2}$ shown in Fig. 4a; these lines separate the region where the thermal barrier can be formed from the region where the barrier cannot be formed because of insufficient pumping in TMX-U. Also shown in Fig. 4a are data points indicating where end plugging was or was not achieved.

Figure 4a also schematically depicts regions where end plugging is either routinely observed or not observed in TMX-U. In addition to collisional trapping, cold ions can be trapped in the thermal barrier by ionization of neutral particles penetrating the plasma; this may account for some of the scattering of data points in Fig. 4a. We infer from Fig. 4a that strong microinstabilities do not exist because large departures from Coulomb processes do not occur. Figure 4a indicates that the path to achieving thermal barriers at higher densities lies in increasing the temperature of passing ions. Central cell ions are heated by ICRF using a Faraday-shielded double-loop antenna excited in an $m = 1$ azimuthal configuration. Each loop subtends a 170° arc around the plasma circumference. Ions have been heated to 2 keV in the perpendicular direction and to 0.4 keV in the parallel direction. In addition, we are also beginning to operate a slot type ICRF antenna located on the other side of the central cell midplane.

Another critical parameter for thermal barrier formation is the fraction of hot mirror confined electrons. For TMX-U, theory [10, 11, 12] predicts that a ratio of $n_{e\text{-}hot}/n_{total} \simeq 0.8$ is required for a confining potential of $\phi_c > 0$. We measured the hot electron temperature for a series of shots with a radiometer and combined our results with diamagnetism measurements to estimate the hot electron density. We measured the total density with a microwave interferometer. Figure 4b depicts our data: the hot electron density data are plotted vs total density data for shots that did and did not achieve end plugging of central cell ions. With the exception of a single entry, the data show that end plugging requires a large fraction of hot electrons. In addition, the shots with end plugging lie close to the theoretical, minimum-required, hot-electron fraction.

REFERENCES

[1] SIMONEN, T.C., et al., Phys. Rev. Lett. **50** (1983) 1668.

[2] ORZECHOWSKI, T. J., S. L. Allen, J. H. Foote, et al., Phys. Fluids **26** (1983) 2335.

[3] GRUBB, D. P., et al., "Thermal Barrier Production and Identification in a Tandem Mirror", Lawrence Livermore National Laboratory, Livermore, CA, UCRL-90536. Accepted for publication in Physical Review Letters.

[4] STALLARD, B. W., et al., (Proc. of 4th International Symposium on Heating in Toroidal Plasmas, Rome, Italy, March 21-28, 1984).

[5] MOLVIK, A. W., et al., (Proc. of 4th International Symposium on Heating in Toroidal Plasmas, Rome, Italy, March 21-28, 1984).

[6] HOOPER, JR., E. B., et al., "Radial transport reduction in tandem mirrors using end wall boundary conditions," Lawrence Livermore National Laboratory, Livermore, CA, UCRL-90639. Accepted for publication in Physics of Fluids.

[7] MOLVIK, A. W., Rev. Sci. Inst. **52** (1981) 704.

[8] COHEN, R. H., and ROWLANDS, G., Phys. Fluids **24** (1981) 2295 and MIRIN, A. A., et al., Nucl. Fusion **23** (1983) 703.

[9] TURNER, W. C., et al., "Gas pressure in the end plug regions of the TMX-U thermal barrier experiment", Lawrence Livermore National Laboratory, Livermore, CA, UCRL-89938, (1983), to be published.

[10] COHEN, R. H., Phys. Fluids **26** (1983) 2774.

[11] MATSUDA, Y. and ROGNLIEN, T. D., Phys. Fluids **26** (1983) 2778.

[12] STALLARD, B. W. et al., Nucl. Fusion **23** (1983) 213.

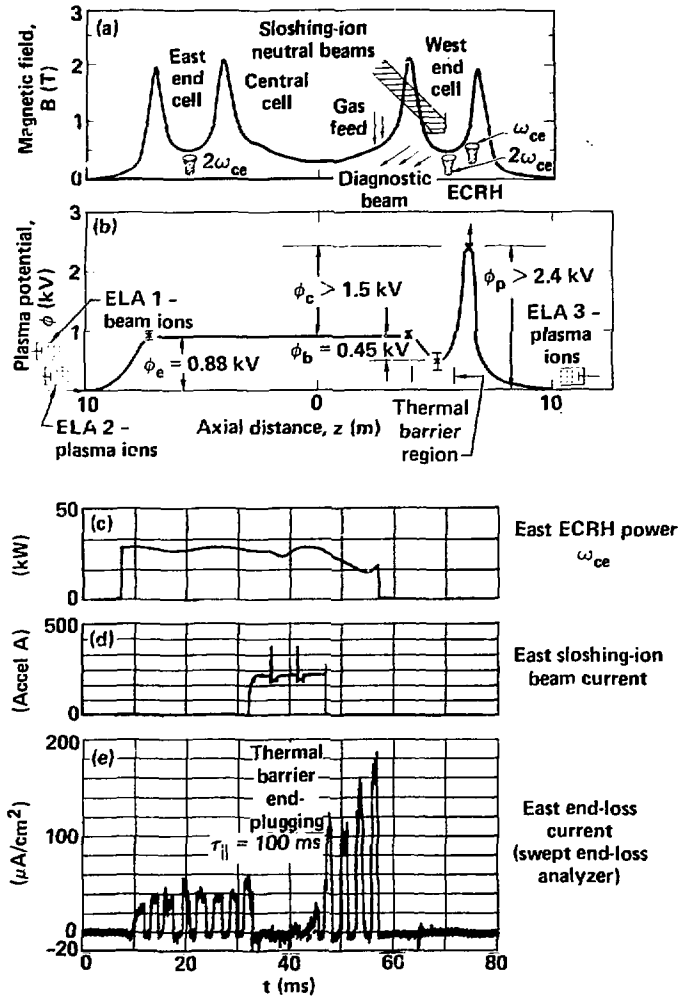

FIG. 1. Thermal barrier measurements in TMX-U: (a) Axial profile of the magnetic field with illustration of the heating systems used for single-end plugging operation; (b) Axial measured potential profile; (c) Time history of ECRH power; (d) Time history of sloshing beam current; (e) Time history of resulting end-loss current measured with a swept end-loss analyzer showing that both ECRH and sloshing beams are required to reduce end losses.

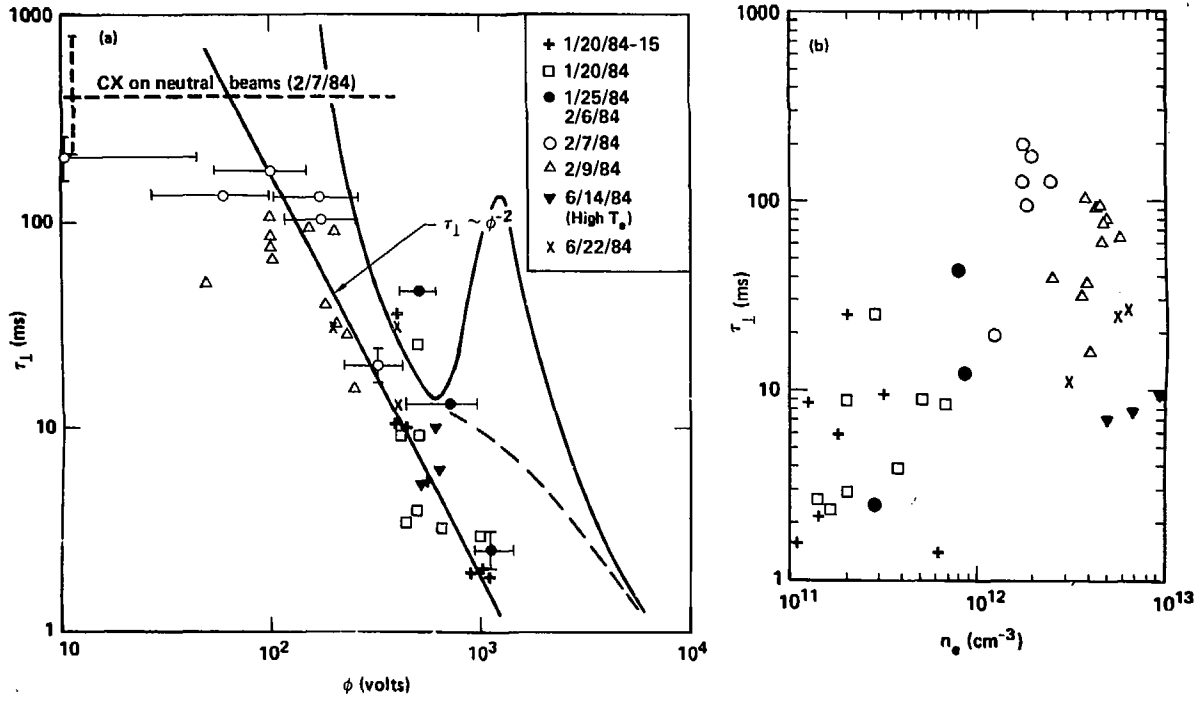

FIG. 2. Scaling of nonambipolar radial ion transport for $r_c \leq 12.9$ cm with (a) central cell potential ϕ_e and (b) density n_c. In part (a), the curved theory line was calculated using $T_i = \phi_e/4$ and the dashed line is a sketch of the expected effects of collisional stochasticty. A line with slope $\tau_\perp \sim \phi^{-2}$ is also shown.

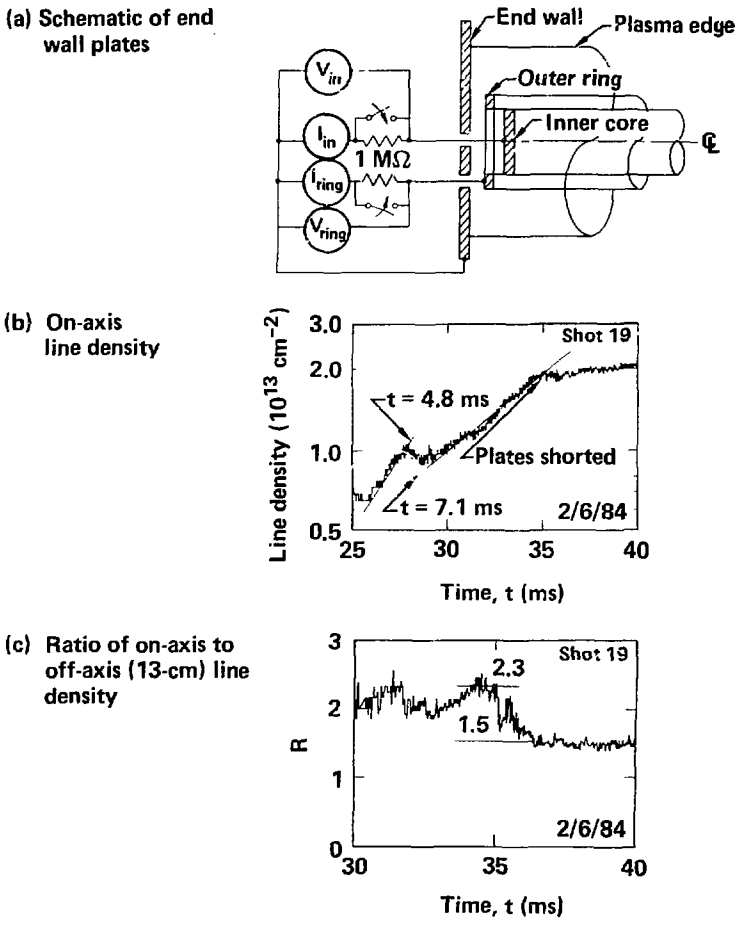

FIG. 3. Plasma behavior using electrically floating end plates: (a) schematic of the end plates, (b) central cell line density vs time with the end plates initially floating and then shorted at t = 35 ms, and (c) ratio (R) of line densities measured on radial chords through r_c = 0 and r_c = 13 cm.

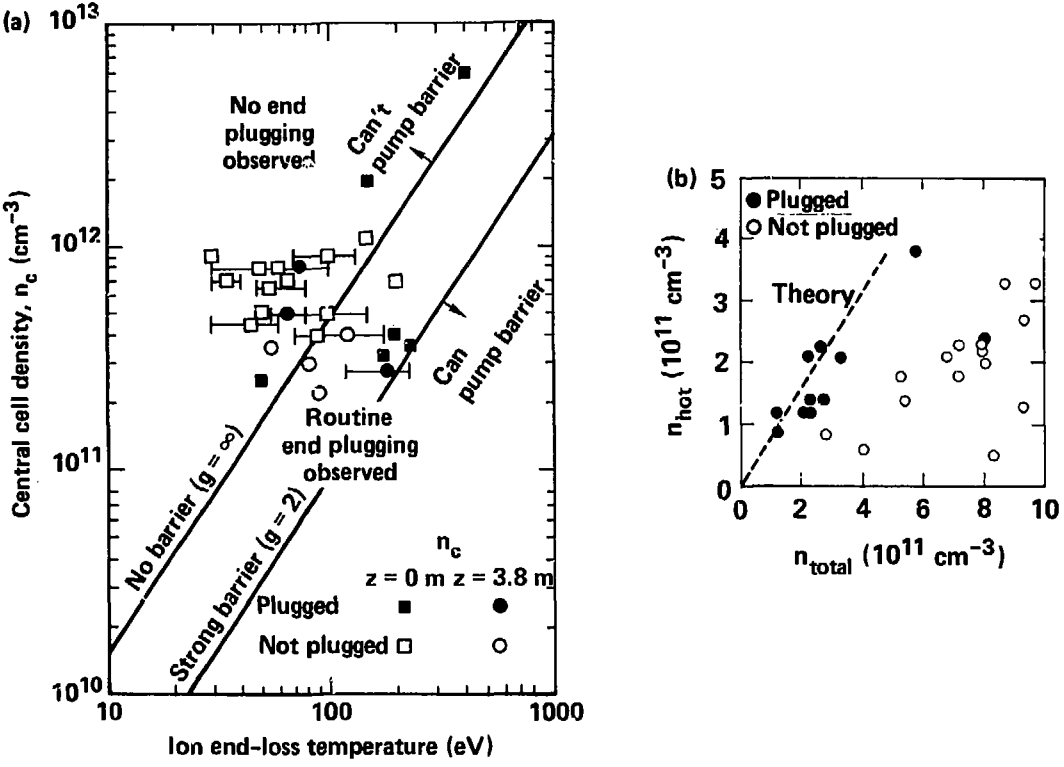

FIG. 4. Thermal barrier scaling curves for: (a) thermal barrier formation vs barrier filling parameters n_c and T_{ic}; and (b) thermal barrier formation vs hot electron fraction.